Combinatorial Materials Research Applied to the Development of New Surface Coatings XIII: An Investigation of Polysiloxane Antimicrobial Coatings Containing Tethered Quaternary Ammonium Salt Groups

Partha Majumdar,[†] Elizabeth Lee,[†] Nathan Gubbins,[†] David A. Christianson,[†] Shane J. Stafslien,[†] Justin Daniels,[†] Lyndsi VanderWal,[†] James Bahr,[†] and Bret J. Chisholm*[,†,‡]

The Center for Nanoscale Science and Engineering, North Dakota State University, 1805 Research Park Drive, Fargo, North Dakota 58102, and Department of Coatings and Polymeric Materials, North Dakota State University, 1735 Research Park Drive, Fargo, North Dakota 58102

Received July 30, 2009

High-throughput biological assays were used to develop structure - antimicrobial relationships for polysiloxane coatings containing chemically bound (tethered) quaternary ammonium salt (QAS) moieties. The QAS-functional polysiloxanes were derived from solution blends of a silanol-terminated polydimethylsiloxane, a trimethoxysilane-functional QAS (QAS-TMS), and methylacetoxysilane. Since the QAS moieties provide antimicrobial activity through interaction with the microorganism cell wall, most of the compositional variables that were investigated were associated with the chemical structure of the QAS-TMS. Twenty different QAS-TMS were synthesized for the study and the antimicrobial activity of sixty unique polysiloxane coatings derived from these QAS-TMS determined toward *Escherichia coli*, *Staphylococcus aureus*, and *Candida albicans*. The results of the study showed that essentially all of the compositional variables significantly influenced antimicrobial activity. Surface characterization of these moisture-cured coatings using atomic force microscopy as well as water contact angle and water contact angle hysteresis measurements indicated that the compositional variables significantly affected coating surface morphology and surface chemistry. Overall, compositional variables that produced heterogeneous surface morphologies provided the highest antimicrobial activity suggesting that the antimicrobial activity was primarily derived from the relationship between coating chemical composition and self-assembly of QAS moieties at the coating/air interface. Using data modeling software, a narrow region of the compositional space was identified that provided broad-spectrum antimicrobial activity.

Introduction

Quaternary ammonium salts (QAS) have been known and widely used for more than half a century to control microbial growth for a variety of applications such as biomedical devices, implants, water cooling systems, wood preservation, fabric treatment, hair rinses, and food products.[1−5] The mechanism by which QAS exert their biocidal activity is a multistep process.[6] The first step of the process is the adsorption of QAS on the surface of the bacterial cell through electrostatic interactions between the negatively charged bacterial cell wall and positively charged QAS. After adsorption onto the surface of the bacterial cell, the QAS diffuse through the cell wall and disrupt the cytoplasmic membrane to release potassium and other constituents which cause cell death.[7,8] The chemical composition of a QAS plays an important role in antimicrobial activity.[9−11] For example, Ahlstrom et al.[12] reported that QAS possessing a long hydrophobic chain affect the outer membrane of Gram-negative bacteria more effectively than shorter-chain analogs due to a stronger interaction of the long alkyl chain with the fatty acid portion of lipid A within the outer membrane.

Tethering (i.e., covalently bonding) QAS to a surface to achieve long-term activity has been previously investigated.[13−15] Surfaces coated with QAS-containing polymers have been shown to be very effective in killing a wide range of microorganisms such as Gram-positive and Gram-negative bacteria, yeasts, and molds.[15−17] Various material architectures such as self-assembled monolayers, polyelectrolyte layers, and hyper-branched dendrimers have been used to produce biocidal surfaces.[18−20] While surface tethered QAS moieties have been shown to exhibit antimicrobial properties, the mechanism of kill must be different than that described for QAS in solution because of diffusion limitations of tethered QAS. Kugler et al.[21] recently reported on the mechanistic aspects of tethered QASs and showed the existence of a charge-density threshold for surfaces bearing tethered QAS groups. To obtain antimicrobial activity, it was concluded that the concentration of surface bound QAS

* To whom correspondence should be addressed. E-mail: Bret.Chisholm@ndsu.edu.
[†] The Center for Nanoscale Science and Engineering.
[‡] Department of Coatings and Polymeric Materials.

10.1021/cc900114e CCC: $40.75
Published on Web 10/06/2009

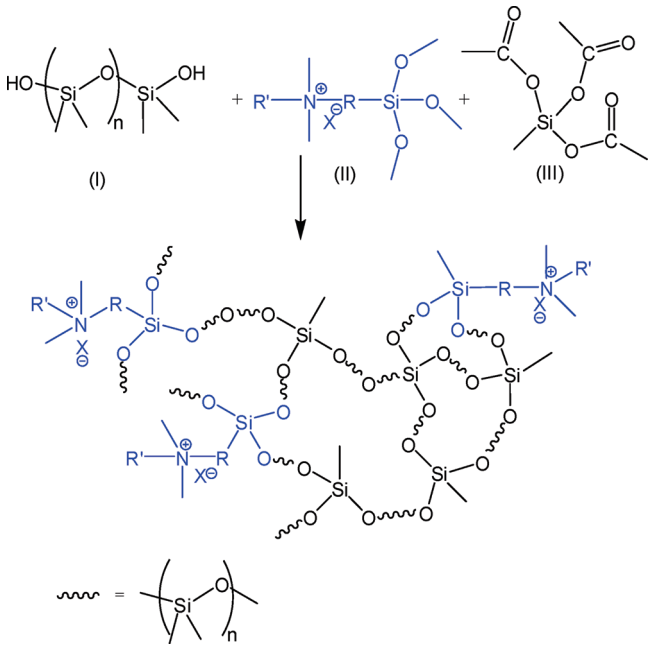

Figure 1. Reaction scheme describing the chemistry associated with the QAS-functional polysiloxane coatings.

groups had to be high enough to cause sufficient cation exchange with cations associated the bacterial membrane to induce disruption of the bacterial envelope. This threshold QAS charge density was found to vary with the species of bacterium, as well as the metabolic state of the bacterium.

Polysiloxanes possessing tethered QAS groups are viewed as being potentially useful antimicrobial surface coatings for various biomedical devices, such as catheters, contact lenses, ophthalmic lenses, and medical implants.[22−26] In general, polysiloxanes have been shown to exhibit biocompatibility, and the ability to introduce antimicrobial properties via the incorporation of covalently bound QAS groups may enable the production of devices that reduce the occurrence of infection. In addition, unlike coatings that release an antibiotic to inhibit infection, these coatings should have a lower potential for producing resistant strains of microorganisms.[3,17]

Sauvet et al.[27] showed that the addition of a polydimethylsiloxane copolymer containing pendant QAS groups to a siloxane elastomer composition provided bactericidal activity toward both Gram-negative and Gram-positive bacteria. Although bactericidal testing of the compositions indicated that diffusion of the QAS-functional polysiloxane copolymers from the elastomer was too low to produce a zone of inhibition, the QAS-functional copolymers were not tethered to the cross-linked elastomer matrix and, thus, could be slowly released from the elastomer over time resulting in a reduction in antimicrobial properties.

As shown in Figure 1, the QAS-functional polysiloxane coatings investigated by the authors were derived from a solution blend of a silanol-terminated polydimethylsiloxane (HO-PDMS-OH) [**I**], QAS-functional trimethoxysilane (QAS-TMS) [**II**], and methyltriacetoxysilane (MeAc) [**III**]. With this coating system, cross-linking and tethering of the QAS groups to the polydimethylsiloxane matrix occurs via condensation reactions involving silanol, methoxysilane, and acetoxysilane groups.[28−30] As is the case for QAS-based compounds in solution, it was expected that antimicrobial activity would be a function of QAS compositional factors such as alkyl substituent composition and counterion composition. In addition to compositional variables associated with the QAS-TMS, other compositional variables such as the molecular weight of the HO-PDMS-OH, relative concentration of the components, and solvent composition were expected to have an effect on antimicrobial properties through their influence of coating surface morphology and chemical composition at the coating/air interface. As a result of the relatively large number of compositional variables and the potential for significant interactions between the variables, a combinatorial/high-throughput approach was taken to determine the structure−antimicrobial activity relationships for this compositional space. The application of a combinatorial/high-throughput approach was also thought to be beneficial for identifying compositions that exhibit broad-spectrum antimicrobial activity, which would be worthy of further investigation and optimization for potential commercialization. While still in its infancy, the application of combinatorial/high-throughput methods for research and development of polymeric coatings has been steadily increasing over the current decade.[31−34]

Experimental Section

Materials. Table 1 provides a description of the starting materials used for the investigation. For microbial characterization assays, tryptic soy (TS) broth supplemented with 2.5% dextrose, minimal medium M63 (dextrose as a carbon source), and RPMI-1640 (pH adjusted to 7.3) were utilized as biofilm growth media (BGM) for *Staphylococcus aureus*, *Escherichia coli*, and *Candida albicans*, respectively. All other reagents were used as received from the vendor.

Synthesis of QAS-TMSs. As shown in Figure 2, QAS-TMS were synthesized by reacting an alkyl amine with a trimethoxysilane-functional alkyl halide in a 0.95:1.00 molar ratio. A representative synthetic procedure is as follows: 4.43 g of N,N-dimethyldecylamine (2.39×10^{-2} moles) and 5.00 g of 3-chloropropyltrimethoxysilane (2.52×10^{-2} moles) were charged to a 20 mL vial. The vial was sealed after purging with nitrogen for 5−10 min and the quaternization reaction carried out at 110 °C for 48 h using magnetic stirring. After cooling the reaction to room temperature, 9.43 g of methanol was added to the vial to produce a 50% (w/w) solution of the QAS-TMS in methanol. The compositional details for each QAS-TMS synthesis are provided in Table 2.

Successful QAS-TMS synthesis was confirmed using proton nuclear magnetic resonance (^{1}H NMR) spectroscopy and mass spectroscopy. For each QAS-TMS, peaks in the ^{1}H NMR spectrum ($CDCl_3$ was used as the lock solvent) at 3.5 ppm ($-N^+-CH_2-$) and 3.3 ppm [$(-N^+-(CH_3)_2$] appeared with a complete disappearance of the dimethylamino protons at 2.2 ppm.

Precursor ion mass spectra of the QAS-TMS were based on precursor ions of 120.8 *m*/*z*. This ion was selected since it was the major ion identified in product ion scans of all the QAS-TMS samples. This ion represents cleavage of the trimethoxysilane group. As shown in Table 3, for all of the QAS-TMS products produced, the *m*/*z* value of the major

Table 1. Materials used for the investigation. PDMS = polydimethylsiloxane

material ID	supplier ID	description	supplier
2K-PDMS	DMS-S15	2,000 g/mol silanol terminated PDMS	Gelest
18K-PDMS	DMS-S27	18,000 g/mol silanol terminated PDMS	Gelest
49K-PDMS	DMS-S35	49,000 g/mol silanol terminated PDMS	Gelest
MeAc	SIM 6519	methyltriacetoxysilane	Gelest
3-bromopropyltrimethoxysilane	3-bromopropyltrimethoxysilane	3-bromopropyltrimethoxysilane	Gelest
3-iodopropyltrimethoxysilane	3-iodopropyltrimethoxysilane	3-iodopropyltrimethoxysilane	Gelest
11-bromoundecyltrimethoxysilane	11-bromoundecyltrimethoxysilane	11-bromoundecyltrimethoxysilane	Gelest
Q14-3-Cl	SIT 7090	tetradecyldimethyl(3-trimethoxysilylpropyl) ammoniumchloride	Gelest
Q18-3-Cl	SIO 6620	octadecyldimethyl(3-trimethoxysilylpropyl) ammoniumchloride	Gelest
3-(*N*,*N*-dimethylaminopropyl) trimethoxysilane	SID 3547	3-(*N*,*N*-dimethylaminopropyl) trimethoxysilane	Gelest
TBAF	1.0 M TBAF	1.0 molar tetrabutylammoniumfluoride in tetrahydrofuran	Aldrich
3-chloropropyltrimethoxysilane	3-chloropropyltrimethoxysilane	3-chloropropyltrimethoxysilane	Aldrich
1-iodooctadecane	1-iodooctadecane	1-iodooctadecane	Aldrich
N,*N*-dimethyldecylamine	*N*,*N*-dimethyldecylamine	*N*,*N*-dimethyldecylamine	Fluka
N,*N*-dimethyldodecylamine	*N*,*N*-dimethyldodecylamine	*N*,*N*-dimethyldodecylamine	Fluka
N,*N*-dimethyltetradecylamine	*N*,*N*-dimethyltetradecylamine	*N*,*N*-dimethyltetradecylamine	Fluka
N,*N*-dimethylhexadecylamine	*N*,*N*-dimethylhexadecylamine	*N*,*N*-dimethylhexadecylamine	Fluka
N,*N*-dimethyloctadecylamine	*N*,*N*-dimethyloctadecylamine	*N*,*N*-dimethyloctadecylamine	TCI America
toluene	toluene	toluene	VWR
MeOH	methanol	methanol	VWR
TBS	tryptic soy broth	tryptic soy broth	VWR
TSA	tryptic soy agar	tryptic soy agar	VWR
LBB	Luria−Bertani broth	Luria−Bertani broth	VWR
LBA	Luria−Bertani agar	Luria−Bertani agar	VWR
YNB	yeast nitrogen broth	yeast nitrogen broth	VWR
YNA	yeast nitrogen agar	yeast nitrogen agar	VWR
RPMI-1640 with L-glutamine (w/o phenol red)	RPMI-1640 with L-glutamine (w/o phenol red)	RPMI-1640 with L-glutamine (w/o phenol red)	VWR
dextrose monohydrate	dextrose monohydrate	dextrose monohydrate	VWR
glycerol	glycerol	glycerol	VWR
NaCl	sodium chloride	sodium chloride	VWR
Dey−Engley (D/E) neutralizing broth	Dey−Engley (D/E) neutralizing broth	Dey−Engley (D/E) neutralizing broth	VWR
crystal violet	crystal violet	crystal violet	VWR
glacial acetic acid	glacial acetic acid	glacial acetic acid	VWR
MIBK	4-methyl-2-pentanone	4-methyl-2-pentanone	Alfa Aesar
DC 3140	DC 3140	commercially available silicone coating	Dow-Corning
Intergard 264	Intergard 264	commercially available epoxy primer	IMPC[a]

[a] IMPC is International Marine and Protective Coatings.

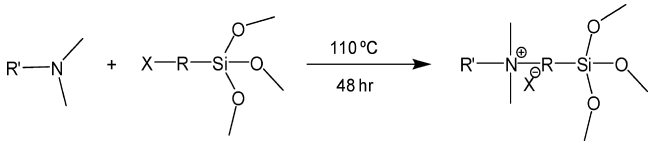

Figure 2. Reaction scheme for the synthesis of QAS-TMS.

precursor ion corresponded to the molecular weight of the desired quaternary ammonium cation, confirming successful synthesis.

Coating Preparation. An automated coating formulation system manufactured by Symyx Discovery Tools, Inc., was used to prepare coating solutions. Materials were dispensed into 20 mL glass vials using a robotic pipet having interchangeable tips and mixed with a magnetic stir bar. Tables 4−6 provide the compositions of each of the coating solutions used for the investigation.

Coating Application. Samples for surface energy measurements, water contact angle hysteresis measurements, and surface morphology characterization were prepared using a Gardco applicator. Drawdowns were made over aluminum panels and curing was achieved by allowing the coatings to lie horizontally for 24 h at ambient conditions followed by a 24 h heat treatment at 50 °C using a VWR Asphalt oven.

For high-throughput measurements involving microorganisms, each coating solution was deposited using an Eppendorf Repeater plus pipetter into a 24-well array plate (6 columns and 4 rows) modified with Intergard 264 epoxy primed aluminum discs in each well. The deposition was done such that a given coating composition occupied an entire column of the 24-well array plate (4 replicate coatings per array plate). The volume of coating solution transferred to each well was 0.25 mL. In addition to experimental coatings, each array plate also contained a silicone reference coating (35 wt % solution of DC 3140 in MIBK). Coatings were allowed to cure for 24 h at room temperature, followed by an additional 24 h at 50 °C.

Instrumentation. ^{1}H NMR spectra were recorded in $CDCl_3$ using a JEOL 400 MHz spectrometer. A sweep width of 7503 Hz was used with 16,000 data points, resulting in an acquisition time of 2.184 s. Sixteen scans were obtained with a relaxation delay of 4 s.

Mass spectrometry measurements were made using an API 4000 quadrupole linear ion trap from Q TRAP, AB/MDS Sciex. 1.0 wt % solutions of QAS-TMSs in methanol were automatically infused directly into the TurboIonSpray source of the mass spectrometer using a CTC Analytics HTS PAL autosampler at a rate of 1 μL/sec (Leap Technologies).

Table 2. Reagents and Weights Used for QAS-TMS Synthesis

QAS	amine reagent	wt (g)	halide reagent[a]	methanol (g)
Q10-3-Cl	*N*,*N*-dimethyldecylamine	4.43	3-chloropropyltrimethoxysilane	9.43
Q12-3-Cl	*N*,*N*-dimethyldodecylamine	5.10	3-chloropropyltrimethoxysilane	10.10
Q14-3-Cl	not synthesized			
Q16-3-Cl	*N*,*N*-dimethylhexadecylamine	6.44	3-chloropropyltrimethoxysilane	11.44
Q18-3-Cl	not synthesized			
Q10-3-Br	*N*,*N*-dimethyldecylamine	3.62	3-bromopropyltrimethoxysilane	8.62
Q12-3-Br	*N*,*N*-dimethyldodecylamine	4.16	3-bromopropyltrimethoxysilane	9.16
Q14-3-Br	*N*,*N*-dimethyltetradecylamine	4.71	3-bromopropyltrimethoxysilane	9.71
Q16-3-Br	*N*,*N*-dimethylhexadecylamine	5.26	3-bromopropyltrimethoxysilane	10.26
Q18-3-Br	*N*,*N*-dimethyloctadecylamine	5.80	3-bromopropyltrimethoxysilane	10.80
Q10-3-I	*N*,*N*-dimethyldecylamine	3.04	3-iodopropyltrimethoxysilane	8.04
Q12-3-I	*N*,*N*-dimethyldodecylamine	3.50	3-iodopropyltrimethoxysilane	8.50
Q14-3-I	*N*,*N*-dimethyltetradecylamine	3.95	3-iodopropyltrimethoxysilane	8.95
Q16-3-I	*N*,*N*-dimethylhexadecylamine	4.42	3-iodopropyltrimethoxysilane	9.42
Q18-3-I	3-(*N*,*N*-dimethylaminopropyl) trimethoxysilane	2.72	1-iodooctadecane	7.72
Q10-11-Br	*N*,*N*-dimethyldecylamine	2.48	11-bromoundecyltrimethoxysilane	7.48
Q12-11-Br	*N*,*N*-dimethyldodecylamine	2.85	11-bromoundecyltrimethoxysilane	7.85
Q14-11-Br	*N*,*N*-dimethyltetradecylamine	3.23	11-bromoundecyltrimethoxysilane	8.23
Q16-11-Br	*N*,*N*-dimethylhexadecylamine	3.60	11-bromoundecyltrimethoxysilane	8.60
Q18-11-Br	*N*,*N*-dimethyloctadecylamine	3.98	11-bromoundecyltrimethoxysilane	8.98

[a] Halide reagent = 5.00 g for each QAS-TMS synthesis.

Table 3. Precursor Ion Mass Spectra Data (*m/z* Values) Data for the QAS-TMS Synthesized

QAS	*m/z*	QAS	*m/z*	QAS	*m/z*	QAS	*m/z*
Q10-3-Cl	348.4	Q10-3-Br	349.2	Q10-3-I	349.3	Q10-11-Br	461.4
Q12-3-Cl	376.6	Q12-3-Br	377.2	Q12-3-I	377.3	Q12-11-Br	489.4
Q14-3-Cl	404.8	Q14-3-Br	405.0	Q14-3-I	405.0	Q14-11-Br	517.6
Q16-3-Cl	432.7	Q16-3-Br	433.0	Q16-3-I	433.4	Q16-11-Br	545.6
Q18-3-Cl	460.7	Q18-3-Br	461.3	Q18-3-I	460.0	Q18-11-Br	573.7

Table 4. Compositions of Coating Solutions Based on 2K-PDMS[a]

Coating	QAS-TMS	Wt. of QAS-TMS soln.
2K-C		
2K-Q10-3-Cl	Q10-3-Cl	0.77
2K-Q12-3-Cl	Q12-3-Cl	0.82
2K-Q14-3-Cl	Q14-3-Cl	0.88
2K-Q16-3-Cl	Q16-3-Cl	0.94
2K-Q18-3-Cl	Q18-3-Cl	0.83
2K-Q10-3-Br	Q10-3-Br	0.86
2K-Q12-3-Br	Q12-3-Br	0.91
2K-Q14-3-Br	Q14-3-Br	0.97
2K-Q16-3-Br	Q16-3-Br	1.03
2K-Q18-3-Br	Q18-3-Br	1.08
2K-Q10-3-I	Q10-3-I	0.95
2K-Q12-3-I	Q12-3-I	1.01
2K-Q14-3-I	Q14-3-I	1.06
2K-Q16-3-I	Q16-3-I	1.12
2K-Q18-3-I	Q18-3-I	1.18
2K-Q10-11-Br	Q10-11-Br	1.11
2K-Q12-11-Br	Q12-11-Br	1.17
2K-Q14-11-Br	Q14-11-Br	1.22
2K-Q16-11-Br	Q16-11-Br	1.28
2K-Q18-11-Br	Q18-11-Br	1.33

[a] All values are in grams. 2K-PDMS = 5.00 g, MeAc = 0.75 g, and Cat soln = 0.75 g were used for each coating solution.

Because of the ionic nature of the QAS-TMS, no acid/base modifiers were necessary to achieve ionization. The ion source parameters were configured as follows: positive polarity, 5500 V ion spray voltage, and configuration for precursor ion scan mode. Precursor ions of *m/z* 120.8 were scanned in quadrupole 1(Q1) from a range of 150−1000 *m/z*. The precursor ion of 120.8 *m/z* was determined to be the major daughter ion during product ion scanning experiments for each QAS-TMS. Prior to infusing each test sample, the infusion line was thoroughly flushed and preconditioned with the new sample. Run time was 3.5 min. Spectra were collected in multiple channel acquisition mode (MCA) for each sample. Data acquisition and analysis was performed using Analyst 1.4.2 software (AB/MDS Sciex).

Table 5. Compositions of Coating Solutions Based on 18K-PDMS[a]

coating	QAS-TMS	wt. of QAS-TMS soln
18K-C		
18K-Q10-3-Cl	Q10-3-Cl	0.77
18K-Q12-3-Cl	Q12-3-Cl	0.82
18K-Q14-3-Cl	Q14-3-Cl	0.88
18K-Q16-3-Cl	Q16-3-Cl	0.94
18K-Q18-3-Cl	Q18-3-Cl	0.83
18K-Q10-3-Br	Q10-3-Br	0.86
18K-Q12-3-Br	Q12-3-Br	0.91
18K-Q14-3-Br	Q14-3-Br	0.97
18K-Q16-3-Br	Q16-3-Br	1.03
18K-Q18-3-Br	Q18-3-Br	1.08
18K-Q10-3-I	Q10-3-I	0.95
18K-Q12-3-I	Q12-3-I	1.01
18K-Q14-3-I	Q14-3-I	1.06
18K-Q16-3-I	Q16-3-I	1.12
18K-Q18-3-I	Q18-3-I	1.18
18K-Q10-11-Br	Q10-11-Br	1.11
18K-Q12-11-Br	Q12-11-Br	1.17
18K-Q14-11-Br	Q14-11-Br	1.22
18K-Q16-11-Br	Q16-11-Br	1.28
18K-Q18-11-Br	Q18-11-Br	1.33

[a] All values are in grams. 18K-PDMS = 5.00 g, MeAc = 0.75 g, and Cat soln = 0.75 g were used for each coating solution.

An automated surface energy measurement unit manufactured by Symyx Discovery Tools, Incorporated and First Ten Angstroms was used to measure coating surface energy (SE) and water contact angle hysteresis (CAH). The method for obtaining SE has been described in detail elsewhere.[35,36] Water CAH was measured using the dispensing/aspirating technique. Advancing contact angle (θ_A) was measured by robotically adding water to a water droplet residing on the coating surface using an addition rate of 0.2 μL/s and monitoring changes in contact angle with time; while receding contact angle (θ_R) was measured by monitoring contact angle as water was withdrawn from the droplet using a withdrawal rate of 0.2 μL/s. The first image was taken after 20 s and subsequent images were taken every 10 s. The total duration of the water addition was 70 s as was the total duration of water removal. θ_A was determined by

Table 6. Compositions of Coating Solutions Based on 49K-PDMS[a]

coating	QAS-TMS	wt. of QAS-TMS soln
49K-C		
49K-Q10-3-Cl	Q10-3-Cl	0.77
49K-Q12-3-Cl	Q12-3-Cl	0.82
49K-Q14-3-Cl	Q14-3-Cl	0.88
49K-Q16-3-Cl	Q16-3-Cl	0.94
49K-Q18-3-Cl	Q18-3-Cl	0.83
49K-Q10-3-Br	Q10-3-Br	0.86
49K-Q12-3-Br	Q12-3-Br	0.91
49K-Q14-3-Br	Q14-3-Br	0.97
49K-Q16-3-Br	Q16-3-Br	1.03
49K-Q18-3-Br	Q18-3-Br	1.08
49K-Q10-3-I	Q10-3-I	0.95
49K-Q12-3-I	Q12-3-I	1.01
49K-Q14-3-I	Q14-3-I	1.06
49K-Q16-3-I	Q16-3-I	1.12
49K-Q18-3-I	Q18-3-I	1.18
49K-Q10-11-Br	Q10-11-Br	1.11
49K-Q12-11-Br	Q12-11-Br	1.17
49K-Q14-11-Br	Q14-11-Br	1.22
49K-Q16-11-Br	Q16-11-Br	1.28
49K-Q18-11-Br	Q18-11-Br	1.33

[a] All values are in grams.49K-PDMS = 5.00 g, MeAc = 0.75 g, Cat soln = 0.75 g, and toluene = 1.25 g were used for each coating solution.

averaging the second to fifth data points during water addition while θ_R was determined by averaging the last four data points. The difference between θ_A and θ_R was reported as the CAH.[37]

Atomic force microscopy (AFM) studies were performed using a Dimension 3100 microscope with a Nanoscope IIIa controller from Veeco Incorporated. Experiments were operated under tapping mode in air at ambient conditions using silicon probes with a spring constant of 0.1−0.4 N/m and resonant frequency of 17−24 kHz. The set point ratio for collection of images was 0.8−0.9.

Software. Design-Expert, version 7.0.3, was used to perform ANOVA analyses, and Spotfire DecisionSite 9.1.1 was used to generate scatter plots.

Microorganisms. The Gram-negative bacterium, *Escherichia coli* ATCC 12435, the Gram-positive bacterium, *Staphylococcus aureus* ATCC 25923, and the opportunistic fungal pathogen, *Candida albicans* ATCC 102321, were received as lyophilized powders and revived in Luria−Bertani (LB) broth, TS broth, and yeast nitrogen (YN) broth + 50 mM dextrose, respectively. Revived bacterial cultures were subcultured twice and stored in frozen 1.0 mL aliquots at −80 °C in the appropriate nutrient broth containing 20 vol % glycerol. The revived culture of *C. albicans* was subcultured twice and stored in frozen 1.0 mL aliquots in the vapor phase of liquid nitrogen in YN broth + 50 mM dextrose containing 20 vol % glycerol. Stocks of *E. coli*, *S. aureus*, and *C. albicans* were maintained weekly at 4 °C on LB, TS, and YN agar plates, respectively.

Antimicrobial Activity of QAS-TMS in Solution. The antimicrobial activity of the QAS-TMSs in solution were evaluated using a combination of methods described previously.[38,39] Broth cultures of *E. coli* and *S. aureus* were prepared by inoculating one colony into 10 mL of broth and incubating at 37 °C with shaking. Overnight cultures were pelleted via centrifugation (10 min at 4500 rpm), washed twice in 0.9 wt % NaCl, and resuspended to a 0.5 McFarland turbidity standard (~10^8 cells ml^{-1}). Two microliters of 50 wt % QAS-TMS in methanol was added to 1 mL of bacterial suspension previously dispensed into a well of a sterile 24-well polystyrene plate. The plates were placed on an orbital shaker and allowed to incubate for 2 h at ambient temperature; 0.1 mL of each QAS-TMS solution/bacterial suspension was immediately transferred to 0.9 mL of Dey/Engley (D/E) neutralization medium in a 1.5 mL microcentrifuge tube and serially diluted (1:10) in D/E medium. Then, 0.2 mL of each dilution was transferred in triplicate to a 96-well plate and incubated statically at 37 °C. After 24 h of incubation, the plates were removed from the incubator and photographed with a digital camera to quantify bacterial growth in solution. Bacterial log reductions were reported as the average of three replicate samples. The bacterial suspensions in 0.9 wt % NaCl (without QAS-TMS addition) served as a positive growth control, while blank D/E medium served as the negative growth control. Methanol was also evaluated for antimicrobial activity as it was used to solubilize the QAS-TMS for biological evaluations.

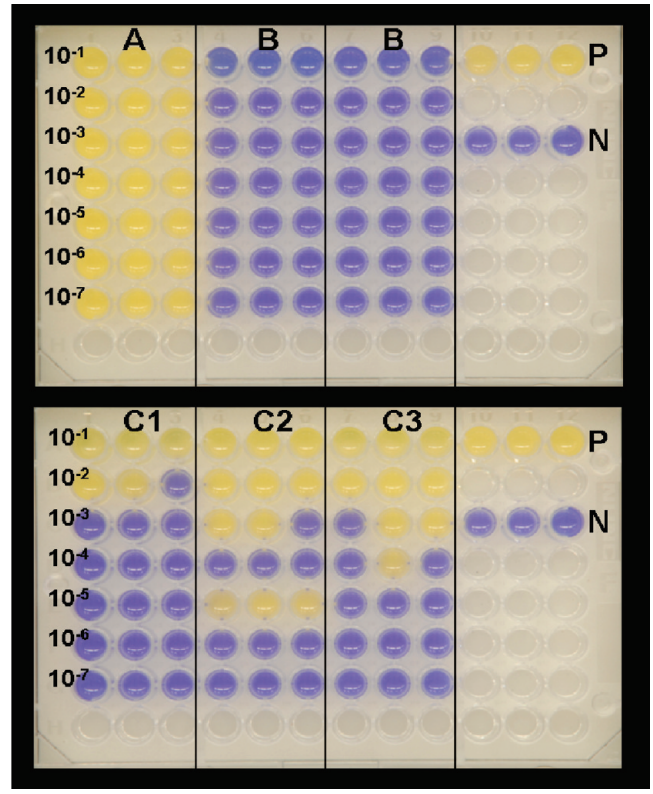

Figure 3. Images of array plates that illustrate representative results obtained from high-throughput screening of antimicrobial activity in aqueous solution. Dilutions are indicated on each row of the plates and three replicate wells were used per dilution (columns). P = bacterial growth in D/E medium (10^{-1} dilution in D/E only); N = no bacterial growth in D/E medium (blank D/E); A = growth in all three replicate wells for each dilution (0 log reduction); B = no growth in all three replicate wells for each dilution (7 log reduction); C = bacterial growth inhibited at different dilutions (C1 = 5.3 log reduction, C2 = 2 log reduction, C3 = 4 log reduction; calculations based on the average of the three replicate wells. Note that C2 was considered positive growth at 10^{-5} for all three replicate wells).

Figure 3 shows representative images of the bacterial growth results obtained in D/E neutralization medium for 6 different QAS-TMS solutions. D/E neutralization medium

contains a pH indicator (bromo cresol purple) that is converted from a purple to yellow color as a consequence of bacterial growth (i.e., utilization of dextrose). This allows for the rapid determination of bacterial log reductions by visual assessment of growth. Three different general results were observed for the QAS-TMS analyzed: (1) bacterial growth evident in each replicate well for each dilution (i.e., 0 log reduction), (2) no bacterial growth in the replicate wells for each dilution (i.e., 7 log reduction), and (3) bacterial growth in one or more of the replicate wells for one or more dilutions. In the case of result 3, the three replicate wells were averaged to obtain a log reduction. D/E neutralization medium was employed in this study to inactivate the antimicrobial activity of the QAS-TMS solution after the initial two hour exposure to the bacterial suspensions.[38] D/E medium will neutralize a variety of disinfectant chemicals and antiseptics including iodine and chlorine preparations, QAS, phenolics, formaldehydes, and glutaraldehydes.[40]

Leachate Toxicity. Prior to the evaluation of microbial biofilm retention, coating array plates were immersed in a recirculating deionized water tank for 67 days to remove any residual toxic components (i.e., catalyst, solvent, unreacted QAS-TMS, etc.) that could potentially leach out and interfere with the biological assays designed to specifically characterize the antimicrobial properties of the coating surfaces.[41] A leachate toxicity assay, which has been previously described in detail, was used to verify that no toxic components were leaching from the coatings after the 67 days of water immersion.[42] Briefly, 1.0 mL of the appropriate BGM was added to each well of the coating array plates and the plates agitated for 24 h at ambient conditions using an orbital shaker (150 rpm). The resultant coating leachates were collected and 0.05 mL of the appropriate microorganism suspension (*E. coli*, *S. aureus*, or *C. albicans*) in BGM ($\sim 10^8$ cells mL^{-1}) was added to 1.0 mL of each coating leachate; 0.2 mL of coating leachate, with the addition of the appropriate microorganism, was transferred in triplicate to a sterile 96-well plate and incubated statically for 24 h at 37 °C. The 96-well plates were subsequently rinsed three times with deionized water and the retained biofilms stained with 0.5 mL of the biomass indicator dye, crystal violet (0.3% alcohol solution), for 15 min. 0.5 mL of 33% glacial acetic acid was added to each coating well to extract the crystal violet dye and absorbance measurements were made at 600 nm with a multiwell plate spectrophotometer. A reduction in bacterial biofilm retention compared to a positive growth control (i.e., organism in fresh growth media) was considered to be a consequence of toxic components being leached from the coating into the overlying medium.

Microbial Biofilm Retention. The rapid evaluation of microbial biofilm retention on coatings prepared in 24-well array plates has been reported previously.[41,43] Briefly, the coated wells of the coating array plates were inoculated with a 1.0 mL suspension of *E. coli*, *S. aureus*, or *C. albicans* in BGM ($\sim 10^7 - 10^8$ cells/mL). The plates were then incubated at 37 °C for 24 (*E. coli* and *C. albicans*) or 48 (*S. aureus*) hours to facilitate cell attachment and biofilm growth within the coated wells. Array plates of coated wells inoculated with *E. coli* and *S. aureus* were incubated statically while array plates inoculated with *C. albicans* were placed on an orbital shaker (150 rpm). The coated wells of each array plate were then rinsed three times with 1.0 mL of deionized water to remove any planktonic or loosely attached biofilm. The biofilm retained on each coating surface after rinsing was then stained with crystal violet dye. Once dry, the array plates were imaged, and the crystal violet dye was extracted from the biofilms with the addition of 0.5 mL of 33% glacial acetic acid for 15 min; 0.15 mL of the resulting eluates was transferred to a 96-well plate and measured for absorbance at 600 nm using a multiwell plate spectrophotometer. The absorbance values were directly proportional to the amount of biofilm retained on the coating surfaces. A custom-modified Tecan EVO Freedom 200 liquid-handling robot was utilized to automate the pipetting steps associated with the extraction of the crystal violet dye from the array plates and the transfer of the resulting eluates to 96-well plates for absorbance measurements.[44]

Table 7. List of the Variables Associated with QAS-TMS

variable	levels
alkyl chain connecting the nitrogen and silicon atoms (R group in Figure 1)	$-(CH_2)_3-$
	$-(CH_2)_{11}-$
alkyl group attached to the nitrogen atom (R′ group in Figure 1)	$-(CH_2)_9CH_3$
	$-(CH_2)_{11}CH_3$
	$-(CH_2)_{13}CH_3$
	$-(CH_2)_{15}CH_3$
	$-(CH_2)_{17}CH_3$
halide counterion (X in Figure 1)	Cl
	Br
	I

Results and Discussion

Antimicrobial Properties of QAS-TMS in Aqueous Solution. On the basis of a large body of prior research pertaining to the use of QAS as disinfectants, it was anticipated that variations in the chemical composition of the QAS-TMS (**II** in Figure 1) would have a significant effect on antimicrobial activity.[13,16,18,42] As a result, prior to the generation of polysiloxane coatings based on QAS-TMS, the antimicrobial activity of the QAS-TMS synthesized for the study was determined in aqueous solution using a high-throughput method. Table 7 provides a list of the QAS-TMS variables investigated and Table 8 provides a description of each of the 20 different QAS-TMS synthesized for the study.

The antimicrobial activity of the QAS-TMS in aqueous solution was measured using the Gram-negative bacterium, *E. coli*, and the Gram-positive bacterium, *S. aureus*. As shown in Figures 4 and 5, antimicrobial activity was dependent on both the chemical structure of the QAS-TMS and the species of bacterium. In general, the QAS-TMS were more active toward *S. aureus* than *E. coli*. Variation in activity based on bacterial species was expected considering the general differences in the cell wall of Gram-positive and Gram-negative bacteria. The cell wall of Gram-positive bacteria mainly consists of peptidoglycan and typically lacks an outer membrane, while the cell wall of Gram-negative bacteria consists of two membranes with the inner membrane being based on phospholipids and the outer membrane

Table 8. Description of the QAS-TMS Synthesized[a]

QAS-TMS	R′	R	X
Q10-3-Cl	$-(CH_2)_9CH_3$	$-(CH_2)_3-$	Cl
Q12-3-Cl	$-(CH_2)_{11}CH_3$	$-(CH_2)_3-$	Cl
Q14-3-Cl	$-(CH_2)_{13}CH_3$	$-(CH_2)_3-$	Cl
Q16-3-Cl	$-(CH_2)_{15}CH_3$	$-(CH_2)_3-$	Cl
Q18-3-Cl	$-(CH_2)_{17}CH_3$	$-(CH_2)_3-$	Cl
Q10-3-Br	$-(CH_2)_9CH_3$	$-(CH_2)_3-$	Br
Q12-3-Br	$-(CH_2)_{11}CH_3$	$-(CH_2)_3-$	Br
Q14-3-Br	$-(CH_2)_{13}CH_3$	$-(CH_2)_3-$	Br
Q16-3-Br	$-(CH_2)_{15}CH_3$	$-(CH_2)_3-$	Br
Q18-3-Br	$-(CH_2)_{17}CH_3$	$-(CH_2)_3-$	Br
Q10-3-I	$-(CH_2)_9CH_3$	$-(CH_2)_3-$	I
Q12-3-I	$-(CH_2)_{11}CH_3$	$-(CH_2)_3-$	I
Q14-3-I	$-(CH_2)_{13}CH_3$	$-(CH_2)_3-$	I
Q16-3-I	$-(CH_2)_{15}CH_3$	$-(CH_2)_3-$	I
Q18-3-I	$-(CH_2)_{17}CH_3$	$-(CH_2)_3-$	I
Q10-11-Br	$-(CH_2)_9CH_3$	$-(CH_2)_{11}-$	Br
Q12-11-Br	$-(CH_2)_{11}CH_3$	$-(CH_2)_{11}-$	Br
Q14-11-Br	$-(CH_2)_{13}CH_3$	$-(CH_2)_{11}-$	Br
Q16-11-Br	$-(CH_2)_{15}CH_3$	$-(CH_2)_{11}-$	Br
Q18-11-Br	$-(CH_2)_{17}CH_3$	$-(CH_2)_{11}-$	Br

[a] R, R′, and X are defined in Figure *1*.

consisting of lipopolysaccharides.[20,45] Previous results have shown that QAS tend to be more effective toward Gram-positive bacteria, such as *S. aureus*, than Gram-negative bacteria, such as *E. coli*.[20]

In general, activity toward *E. coli* decreased with an increase in the length of the alkyl chain attached to the nitrogen atom (R′ in Figure 1) and QAS-TMSs with R = $-(CH_2)_3-$ were found to be more active than analogous QAS-TMS with R = $-(CH_2)_{11}-$. Variations as a function of counterion composition were observed for QAS-TMS possessing R′ = $-(CH_2)_{13}CH_3$; however, for QAS-TMS possessing R′ = $-(CH_2)_{13}CH_3$ and R = $-(CH_2)_3-$, maximum antimicrobial activity (i.e., 7 log reduction) was observed independent of counterion composition. Complex relationships between QAS chemical composition and antimicrobial activity, such as those shown in Figure 4, have been previously observed by several investigators.[46−48] For example, Gilbert et al.[46] and Kourai et al.[47] reported a parabolic relationship between R' and antimicrobial activity. Gilbert et al.[46] observed maximum antimicrobial activity toward *S. aureus*, *Saccharomyces cerevisiae*, and *Pseudomonas aeruginosa* for alkyl trimethylammonium bromides possessing 10 and 12 carbon alkyl chains. A similar observation was reported by Kourai et al.[47] for *N*-alkyl-α-methylpyridinium iodides, *N*-alkyldimethylphenylammonium iodides, *N*-alkyltrimethylammonium iodides, *N*-alkylquinolinium iodides, and *N*-alkyl-*iso*-quinolinium iodides toward *E. coli* and *Bacillus subtilis* var. *niger*. In general, the dependence of antimicrobial activity on QAS chemical structure can be attributed to the interplay between several factors such as the affinity of the QAS toward the cell membrane, aggregational behavior of the QAS in solution, steric interactions, and the diffusivity of the QAS through the cell wall. The results shown in Figure 4 indicate a general trend in which QAS-TMS possessing the highest hydrocarbon content exhibit the lowest antimicrobial activity. A higher hydrocarbon content for these amphiphilic compounds would be expected to result in a greater thermodynamic driving force for the formation of aggregates or micelles in aqueous solution thereby reducing antimicrobial effectiveness.

Polysiloxane Coatings Containing Tethered QAS Groups. After synthesizing and evaluating the antimicrobial activity of the QAS-TMS, coatings were produced by solution blending with a HO-PDMS−OH (**I** in Figure 1), MeAc (**III** in Figure 1)), and a catalyst solution to form a "moisture-cure" coating system. The compositional space used for the study was derived from the twenty different QAS-TMS and three different HO-PDMS-OHs that varied with respect to molecular weight. The concentration of QAS-TMS and MeAc were kept constant resulting in a total of 60 unique coating compositions. The responses measured using high-throughput methods included surface properties, namely, SE and water CAH, as well as antimicrobial properties.

Surface Properties. Figures 6 and 7 display SE and water CAH data, respectively, for the coatings prepared. In addition to data for the QAS-containing coatings, data for control coatings (2K-C, 18K-C, and 49K-C) were included and are illustrated by the dashed lines. From Figure 6, it can be seen

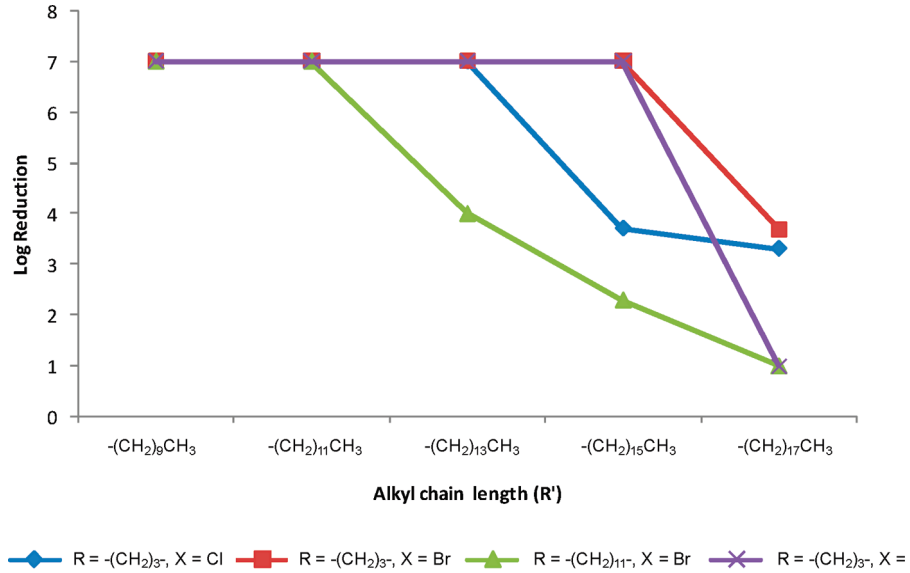

Figure 4. Plot illustrating the antimicriobial activity of the QAS-TMS toward *E. coli*.

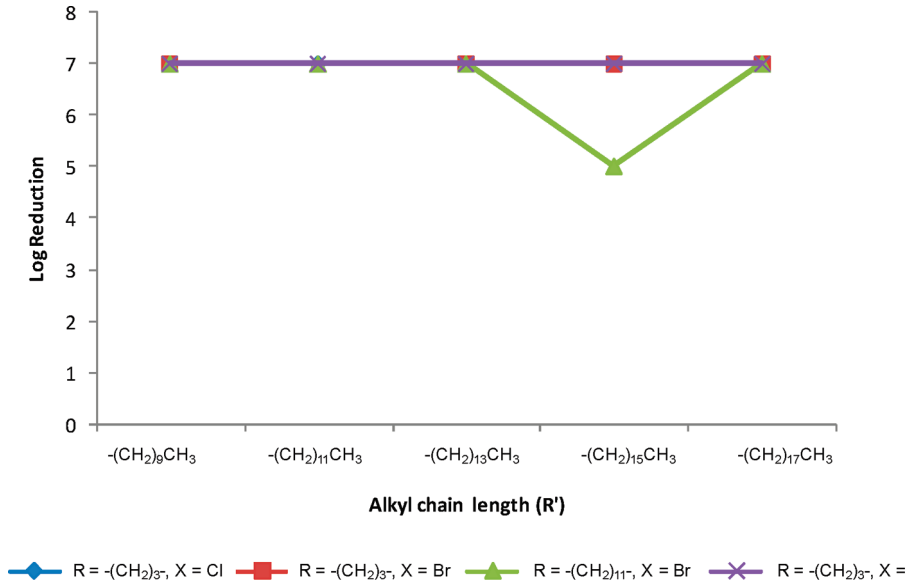

Figure 5. Plot illustrating the antimicriobial activity of the QAS-TMS toward *S. aureus*.

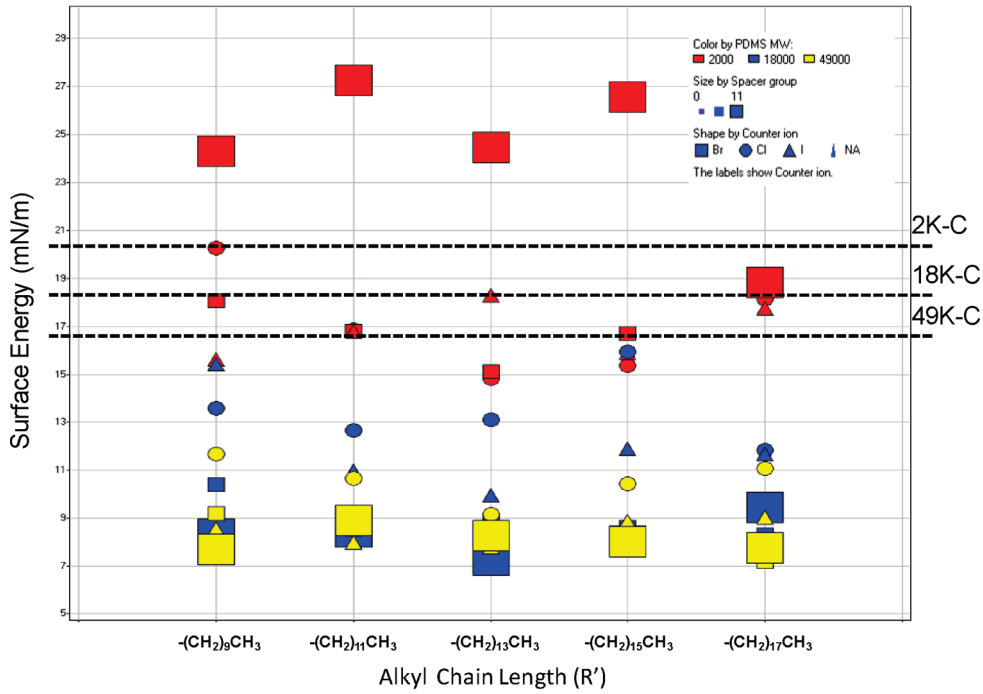

Figure 6. Surface energies measured for the QAS-functional polysiloxane coatings.

that SEs varied dramatically from 7.2 to 27.3 mN/m. Polysiloxane coatings are known for their low SE. Interestingly, most of the QAS-containing coatings possessed a lower SE than the control coatings despite the hydrophilic nature of the QAS functional groups. As discussed in a previous publication,[42] this result can be attributed to a heterogeneous surface morphology comprised of QAS-rich surface protrusions that reduce wetting. In general, the coatings that exhibited SEs ≥ the PDMS control coatings and water CAH values ≤ the PDMS controls were derived from the lowest molecular weight HO-PDMS-OH. This result indicated that the lower molecular weight HO-PDMS−OH, which would result in the highest cross-link densities, produced the most homogeneous, stable surfaces.

To obtain a better understanding of the SE and water CAH results, AFM was conducted on coatings that possessed systematic variations in composition. Figure 8 displays AFM images that illustrate the effect of HO-PDMS−OH molecular weight on surface morphology. The coatings based on the lowest HO-PDMS-OH molecular weight (i.e., 2000 g/mol) had homogeneous surface morphologies while those based on higher HO-PDMS-OH molecular weights (i.e., 18 000 and 49 000 g/mol) formed two-phase, heterogeneous surfaces. The AFM images shown in Figure 9 indicate a trend in surface morphology with the length of the alkyl chain connecting the silicon atom and nitrogen atom of the QAS (R in Figure 1). With the exception of coatings based on R′ = $-(CH_2)_{17}CH_3$, all other coatings based on R = $-(CH_2)_3-$ possessed a heterogeneous surface morphology, while those based on R = $-(CH_2)_{11}-$ displayed a homogeneous surface morphology. On the basis of the previous published results that showed that a heterogeneous surface morphology

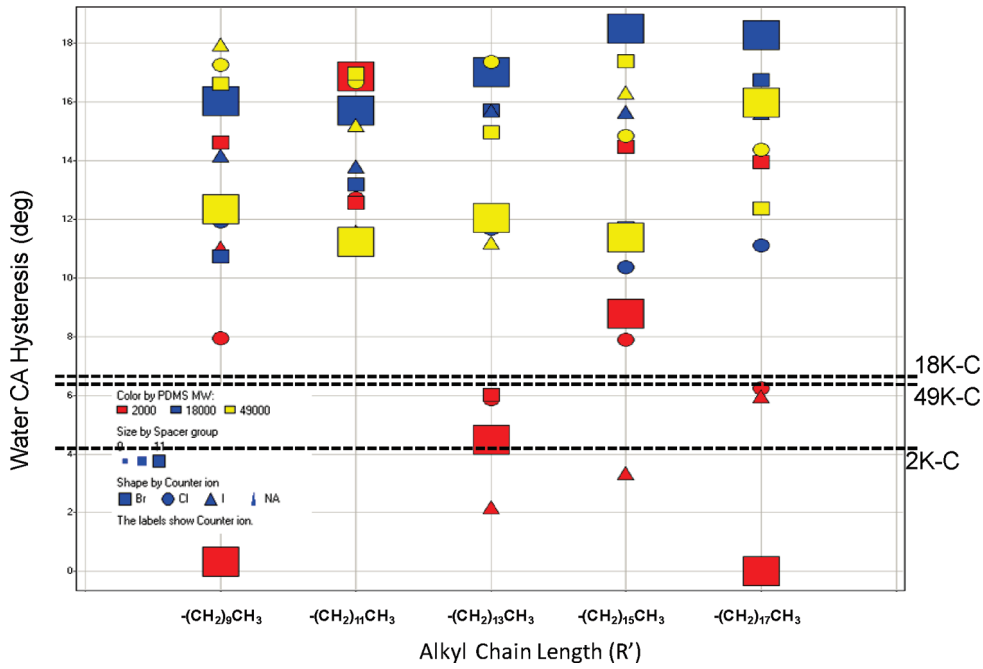

Figure 7. Water contact angle hysteresis values measured for the QAS-functional polysiloxane coatings.

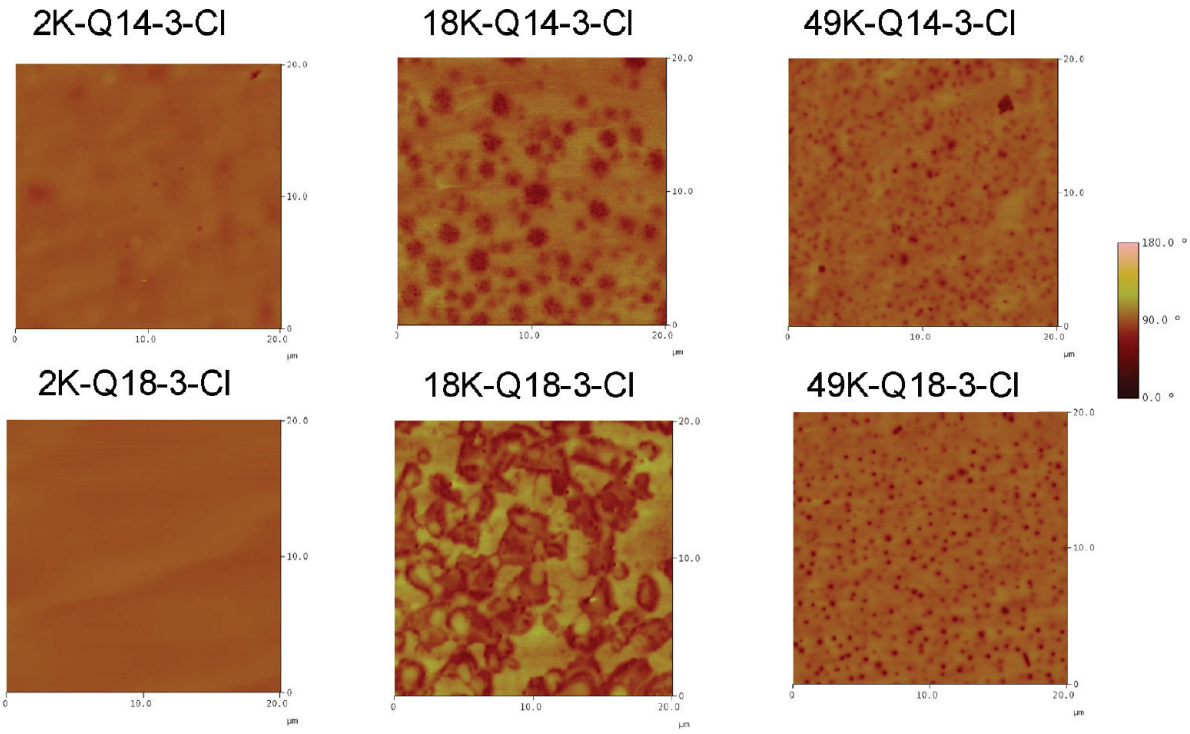

Figure 8. AFM phase images that illustrate the effect of HO-PDMS-OH molecular weight on coating surface morphology.

corresponded to a higher QAS surface concentration, this result indicates that decreasing the hydrophilic−lipophilic balance of the QAS-TMS by increasing R from $-(CH_2)_3-$ to $-(CH_2)_{11}-$ reduces the thermodynamic driving force for segregation of the QAS groups to the coating-air interface.[42]

Antimicrobial Properties of Coatings. Antimicrobial activity was measured using a high-throughput technique that involves quantification of the amount of biomass adhered to coating surfaces using a colorimetric assay.[41,43] The amount of biomass adhered to a coating surface was expressed as a relative reduction compared to a control coating that did not contain QAS functionality. Figures 10−12 display antimicrobial activity toward *E. coli*, *S. aureus*, and *C. albicans*, respectively. The figures are scatter plots that display variations in all of the factors used for the experiment. The *x*-axis is the variation in R′ of the QAS-TMS, the color of the data symbols indicate variation in HO-PDMS-OH molecular weight, the size of the data symbols indicate variation in R of the QAS-TMS, and the shape of the data symbols indicate variation in QAS-TMS counterion. From the data shown in Figures 10−12, a wide variation in antimicrobial activity can be observed as a function of the compositional variables. A very obvious general trend in the data involves the effect of the composition of the R group of the QAS-

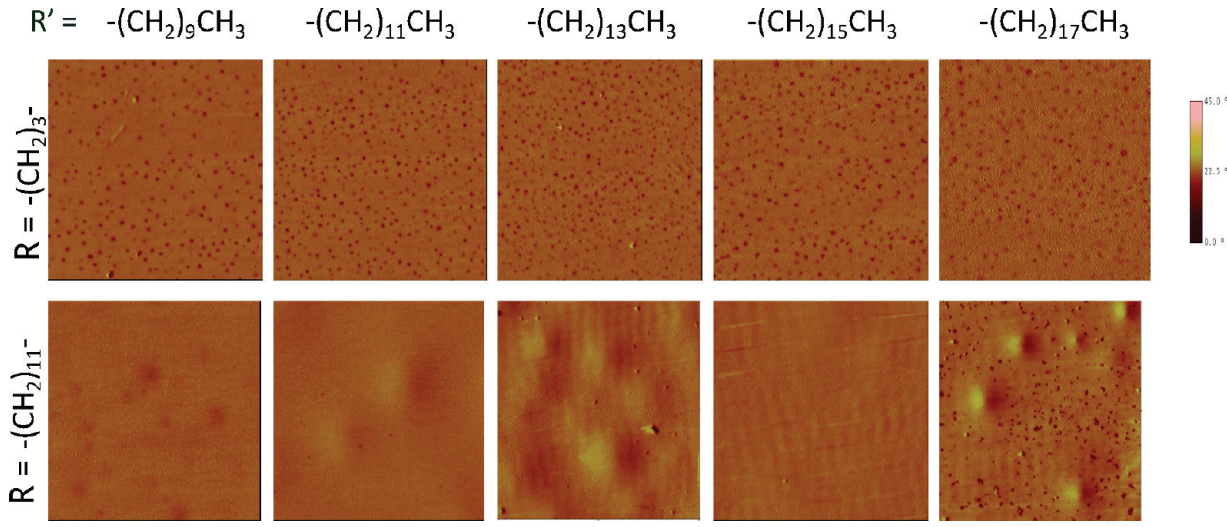

Figure 9. Phase images for coatings derived from 49 000 g/mol HO-PDMS-OH and QAS-TMS possessing a bromine counterion. The images corresponding to a 20 μm × 20 μm area.

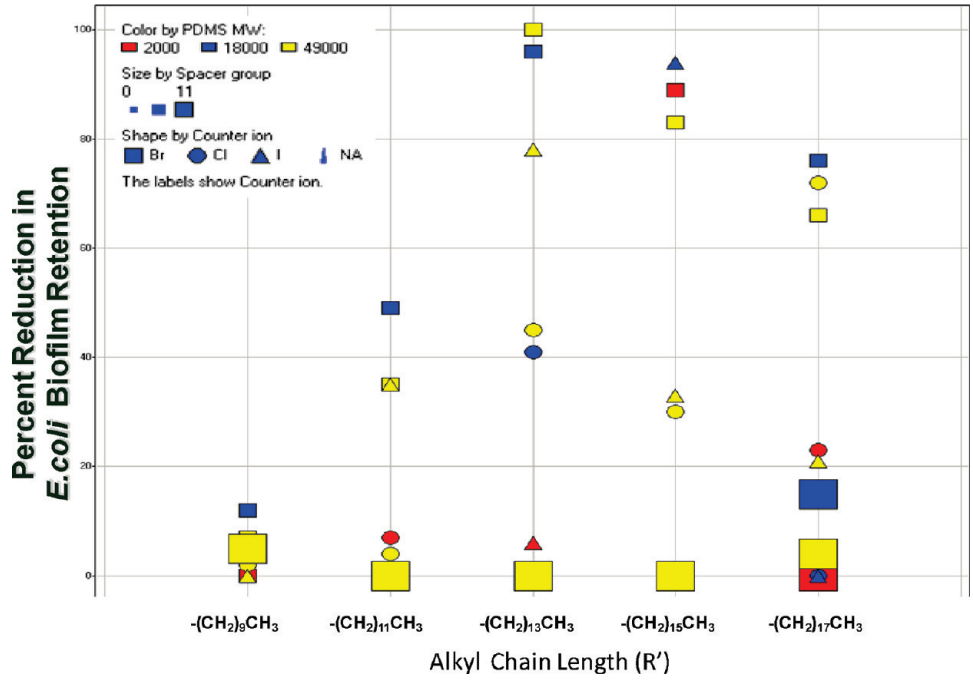

Figure 10. Antimicrobial activity of the coatings toward *E. coli.*

TMS. Compositions based on the relatively short R group (i.e., -$(CH_2)_3$-) generally showed significantly higher antimicrobial activity than analogous compositions based on the relatively long R group (i.e., -$(CH_2)_{11}$-). This result is consistent with the AFM results and the authors' previously reported results and indicated a higher concentration of QAS functionality at the coating surface for coatings based on R = $-(CH_2)_3-$.[42]

To identify other statistically significant trends in the antimicrobial data, an ANOVA analysis was performed and the results are provided in Table 9. For each response, the *p* value of the model was less than 0.003, which indicated that the overall model was significant. For each microorganism, at least two different coating compositional variables had a significant effect on antimicrobial activity; however, the significant factors were not consistent between microorganisms. For example, HO-PDMS-OH molecular weight, QAS-TMS R group composition, and QAS-TMS counterion composition (X) significantly affected the antimicrobial activity of the Gram-negative bacterium, *E. coli*, while QAS-TMS R and R′ composition were the only significant compositional factors for the antimicrobial activity of the Gram-positive bacterium, *S. aureus*. For the opportunistic fungal pathogen, *C. albicans*, QAS-TMS R group and counterion composition were significant as was an interaction between HO-PDMS−OH molecular weight and R group composition. Considering the vast differences in cell biology for the three different microorganisms utilized for the study, variations in antimicrobial activity as a function of the species of microorganism was expected.[49,50]

A comparison of the antimicrobial activity data obtained for QAS-TMS compounds in aqueous solution to antimicrobial activity data obtained for QAS-containing coatings indicated that solution activity data was a poor predictor of

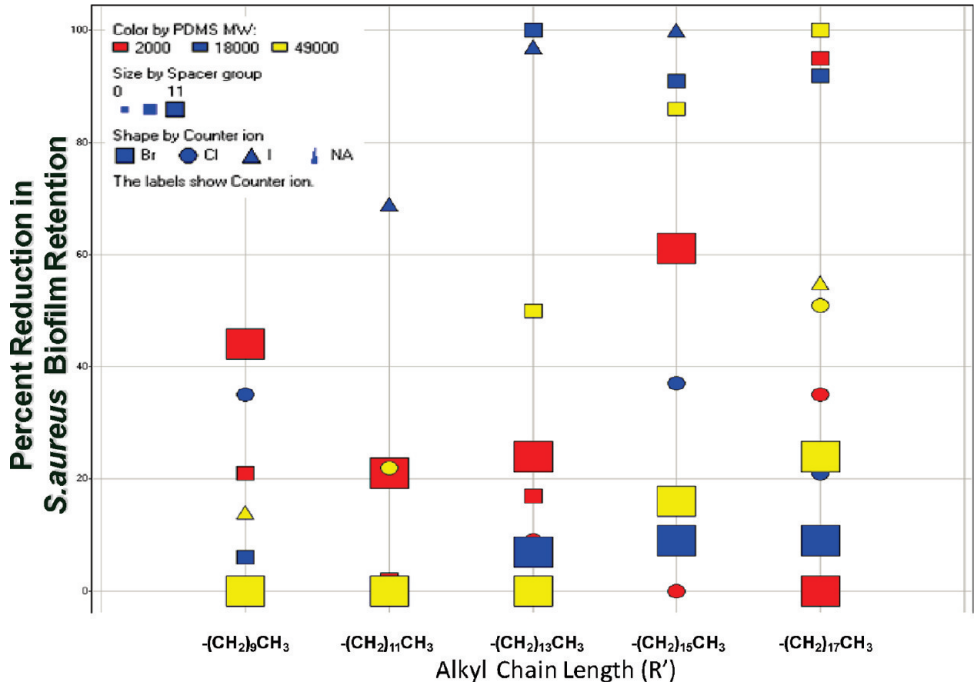

Figure 11. Antimicrobial activity of the coatings toward *S. aureus.*

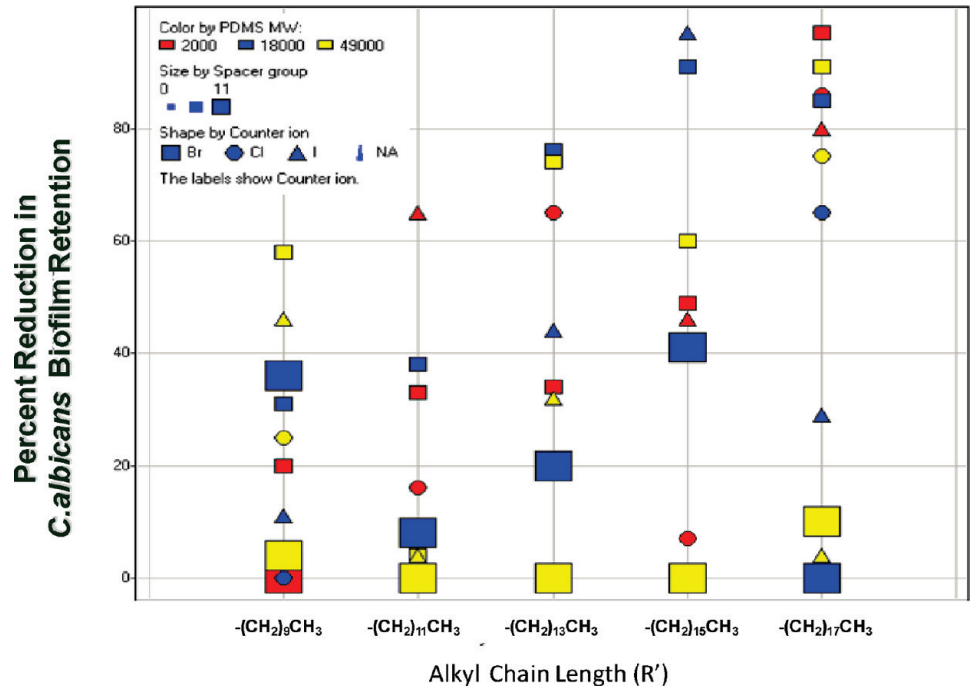

Figure 12. Antimicrobial activity of the coatings toward *C. albicans.*

antimicrobial activity of the surface coatings. For example, all of the QAS-TMS compounds possessing R′ = −$(CH_2)_9CH_3$ displayed 7 log reduction toward *E. coli* in aqueous solution independent of the composition of the R group or counterion, while polysiloxane coatings based on these QAS-TMS showed little or no antimicrobial activity. This result further illustrates that the antimicrobial activity of the coatings is highly dependent on the influence of compositional variables on surface morphology. To obtain an antimicrobial coating, it is a prerequisite that the QAS groups sufficiently segregate to the coating-air interface.

Although the structure−antimicrobial relationships for the compositional space investigated are rather complex, the data obtained allowed for the identification of compositions that exhibit broad-spectrum antimicrobial activity. Using Design-Expert, the region of the compositional space predicted to provide maximum, broad-spectrum antimicrobial activity was identified. According to the data models, coating compositions derived from R = −$(CH_2)_3$−, R′ = −$(CH_2)_{15}CH_3$, X = Br, and HO-PDMS-OHs ≥ 18 000 g/mol provide maximum reduction in biofilm retention toward all three microorganisms.

Table 9. ANOVA Results for the Antimicrobial Activity of the Coatings[a]

	responses		
terms	% reduction in *E. coli* biofilm retention	% reduction in *S. aureus* biofilm retention	% reduction in *C. albicans* biofilm retention
Model	0.0001	0.0028	0.0001
PDMS	0.0006	0.6684	0.3035
R′	0.0572	0.0014	
R	0.0001	0.0368	0.0001
X	0.0242	0.1382	0.0010
(PDMS)(R)			0.0160

[a] The values listed in the table are *p*-values (Prob > F, i.e., probability of seeing the observed F value if the null hypothesis is true). *p*-value less than 0.05 indicates that the model term is significant.

Conclusion

With regard to structure−antimicrobial relationships, the results of the study indicated that the relationship between coating compositional variables and antimicrobial activity was primarily controlled by the process of self-assembly of QAS moieties to the coating/air interface. The single compositional factor that was found to have a significant effect on antimicrobial activity toward all three microorganisms was the length of the alkyl chain connecting the nitrogen and silicone atoms of the QAS-TMS (R in Figure 1). Decreasing R from $-(CH_2)_{11}-$ to $-(CH_2)_3-$ increased antimicrobial activity toward all three microorganisms. This decrease in R length also corresponded to the production of a heterogeneous microscale surface morphology which, based on previous results, can be attributed to the formation of QAS-rich surface domains.

The application of a high-throughput/combinatorial approach allowed for four different compositional factors to be concurrently varied and the antimicrobial activity toward three different microorganisms to be measured. This capability allowed for an optimum compositional space to be identified that provided broad-spectrum antimicrobial activity. Coating compositions derived from $R = -(CH_2)_3-$, $R' = -(CH_2)_{15}CH_3$, X = Br, and HO-PDMS-OHs ≥ 18 000 g/mol were determined to provided greater than 80% reduction in biofilm retention toward all three microorganisms. Coatings possessing compositions within this narrower compositional space will be investigated further for potential application as an antimicrobial coating for biomedical devices such as urinary catheters.

Acknowledgment. The authors acknowledge financial support from the Office of Naval Research under grants N00014-05-1-0822 and N00014-06-1-0952.

References and Notes

(1) Games, L. M.; King, J. E.; Larson, R. J. *Environ. Sci. Technol.* **1982**, *16*, 483–488.
(2) van Ginkel, C. G. *Chemosphere* **1991**, *23* (3), 281–289.
(3) Gottenbos, B.; Busscher, H. J.; van der Mei, H. C.; Nieuwenhuis, P. *J. Mater. Sci.: Mater. Med.* **2002**, *13* (8), 717–722.
(4) Nishihara, T.; Okamoto, T.; Nishiyama, N. *J. Appl. Microbiol.* **2000**, *88*, 641–647.
(5) Laopaiboon, L.; Hall, S. J.; Smith, R. N. *J. Appl. Microbiol.* **2002**, *93*, 1051–1058.
(6) Tashiro, T. *Macromol. Mater. Eng.* **2001**, *286*, 63–87.
(7) Davies, A.; Bentley, M.; Field, B. S. *J. Appl. Bacteriol.* **1968**, *31* (4), 448–61.
(8) Juergensen, L.; Busnarda, J.; Caux, P.-Y.; Kent, R. A. *Environ. Toxicol.* **2000**, *15* (3), 174–200.
(9) Tomlinson, E.; Brown, M. R. W.; Davis, S. S. *J. Med. Chem.* **1977**, *20*, 1277–1282.
(10) Ioannou, C. J.; Hanlon, G. W.; Denyer, S. P. *Antimicrob. Agents Chemother.* **2007**, *51* (1]?>),]?>), 296–306.
(11) Patel, R. N.; Singh, N.; Gundla, V. L. N.; Chauhan, U. K. *Spectrochim. Acta, Part A* **2007**, *66A* (3), 726–731.
(12) Ahlstrom, B.; Thompson, R. A.; Edebo, L. *Acta. Pathol. Microbiol. Immunol. Scand.* **1999**, *107*, 318–324.
(13) Hazziza-Laskar, J.; Helary, G.; Sauvet, G. *J. Appl. Polym. Sci.* **1995**, *58*, 77–84.
(14) Cheng, B.; Wang, Y.; Du, Q. *J. Appl. Polym. Sci.* **2005**, *96* (5), 1847–1854.
(15) Pant, R. R.; Buckley, J. L.; Fulmer, P. A.; Wynne, J. H.; McCluskey, D. M.; Phillips, J. P. *J. Appl. Polym. Sci.* **2008**, *110*, 3080–3086.
(16) Sauvet, G.; Fortuniak, W.; Kazmierski, K.; Chojnowski, J. *J. Polym. Sci., Part A: Polym. Chem.* **2003**, *41* (19), 2939–2948.
(17) Gottenbos, B.; van der Mei, H. C.; Klatter, F.; Nieuwenhuis, P.; Busscher, H. J. *Biomaterials* **2002**, *23* (6), 1417–1423.
(18) Thebault, P.; Taffin de Givenchy, E.; Guittard, F.; Guimon, C.; Geribaldi, S. *Thin Solid Films* **2008**, *516* (8), 1765–1772.
(19) Wang, Y.; Dubin, P. L *J. Chromatogr., A.* **1998**, *808* (1−2), 61–70.
(20) Chen, C. Z.; Beck-Tan, N. C.; Dhurjati, P.; Van Dyk, T. K.; LaRossa, R. A.; Cooper, S. L *Biomacromolecules* **2000**, *1* (3), 473–480.
(21) Kuegler, R.; Bouloussa, O.; Rondelez, F. *Microbiology* **2005**, *151* (5), 1341–1348.
(22) Green, T. R.; Fellman, J. U. S. Patent 6,939,569, 2005.
(23) Green, T. R.; Fellman, J. PCT Int. Appl. WO 9,965,538, 1999.
(24) Robertson, J. R. Eur. Pat. Appl. EP 611782, 1994.
(25) Valint, P. L.; Mcgee, J. A.; Vanderbilt, D. P. U. S. Pat. Appl. Publ. US 2007116741, 2007.
(26) Moss, H. A.; Tebbs, S. E.; Faroqui, M. H.; Herbst, T.; Isaac, J. L.; Brown, J.; Elliott, T. S. J. *Eur. J. Anaesthesiol.* **2000**, *17* (11), 680–687.
(27) Sauvet, G.; Dupond, S.; Kazmierski, K.; Chojnowski, J. *J. Appl. Polym. Sci.* **2000**, *75* (8), 1005–1012.
(28) Andersson, L. H. U.; Hjertberg, T. J. *J. Appl. Polym. Sci.* **2003**, *88*, 2073–2081.
(29) Arkles, B. *CHEMTECH* **1977**, *7* (12), 766–778.
(30) Kahn, F. *Appl. Phys. Lett.* **1973**, *22* (8), 386–388.
(31) Chisholm, B.; Potyrailo, R.; Cawse, J.; Shaffer, R.; Brennan, M.; Molaison, C. *Prog. Org. Coat.* **2003**, *47*, 120–127.
(32) Chisholm, B.; Potyrailo, R.; Cawse, J.; Shaffer, R.; Brennan, M.; Molaison, C.; Whisenhunt, D.; Flanagan, B.; Olson, D.; Akhave, J.; Saunders, D.; Mehrabi, A.; Licon, M. *Prog. Org. Coat.* **2002**, *45*, 313–321.
(33) Webster, D. C.; Chisholm, B. J.; Stafslien, S. J. *Biofouling* **2007**, *23*, 179–192.
(34) Webster, D. C.; Bennett, J.; Kuebler, S.; Kossuth, M. B.; Jonasdottir, S. *JCT Coatings Tech* **2004**, *1* (6), 34–39.
(35) Correia, N. T.; Moura Ramos, J. J.; Saramago, B. J. V.; Calado, J. C. G. *J. Colloid Interface Sci.* **1997**, *189*, 361–369.

(36) Owens, D. K.; Wendt, R. D. *J. Appl. Polym. Sci.* **1969**, *13*, 1741–1747.
(37) Majumdar, P.; Stafslien, S.; Daniels, J.; Webster, D. C. *J. Coat. Technol. Res.* **2007**, *4* (2), 131–138.
(38) Dey, B. P.; Engley, F. B. *J. Ind. Microbiol.* **1995**, *14*, 21–25.
(39) Ramesh, R.; Rasley, B. T.; Buckley, J. P.; Lloyd, C. T.; Cozzens, R. F.; Santangelo, P. G.; Wynne, J. H. *J. Appl. Polym. Sci.* **2007**, *104*, 2954–2964.
(40) Voiget Global Distribution. http://www.voigtglobal.com/Anonymous/Difco_Hycheck_Products.pdf (accessed July2009)
(41) Stafslien, S. J.; Bahr, J. A.; Feser, J. M.; Weisz, J. C.; Chisholm, B. J.; Ready, T. E.; Boudjouk, P. *J. Combi. Chem.* **2006**, *8* (2), 156–162.
(42) Majumdar, P.; Lee, E.; Patel, N.; Ward, K.; Stafslien, S. J.; Daniels, J.; Chisholm, B. J.; Boudjouk, P.; Callow, M. E.; Callow, J. A.; Thompson, S. E. M. *Biofouling* **2008**, *24* (3), 185–200.
(43) Stafslien, S.; Daniels, J.; Chisholm, B.; Christianson, D. *Biofouling* **2007**, *23* (1/2), 37–44.
(44) Kugel, A. J.; Jarabek, L. E.; Daniels, J. W.; Vander Wal, L. J.; Ebert, S. M.; Jepperson, M. J.; Stafslien, S. J.; Pieper, R. J.; Webster, D. C.; Bahr, J.; Chisholm, B. J. *J. Coat. Technol. Res.* **2009**, *6* (1), 107–121.
(45) Dubnickova, M.; Rezanka, T.; Koscova, H. *Folia Microbiol.* **2006**, *51* (5), 371–374.
(46) Gilbert, P.; Al-Taae, A. *Lett. Appl. Microbiol.* **1985**, *1*, 101–104.
(47) Kourai, H.; Horie, T.; Takeichi, K.; Shibasaki, I. *J. Antibact. Antifung. Agents* **1980**, *8*, 9–17.
(48) Majumdar, P.; Lee, E.; Gubbins, N.; Stafslien, S. J.; Daniels, J.; Thorson, C. J.; Chisholm, B. J. *Polymer* **2009**, *50* (5), 1124–1133.
(49) Russell, A. D. *J. Infect. Dis.* **1993**, *168*, 1339–1340.
(50) Russell, A. D. *Int. Biodeterior. Biodegrad.* **1995**, *36* (3/4), 247–265.

CC900114E